ORIGINAL RESEARCH

In vivo Ca²⁺ dynamics induced by Ca²⁺ injection in individual rat skeletal muscle fibers

Mario Wakizaka[1], Hiroaki Eshima[1,2], Yoshinori Tanaka[1], Hideki Shirakawa[1], David C. Poole[3] & Yutaka Kano[1]

1 Department of Engineering Science, Bioscience and Technology Program, University of Electro-Communications, Chofu, Tokyo, Japan
2 Department of Metabolism and Endocrinology, Juntendo University Graduate School of Medicine, Hongo, Tokyo, Japan
3 Departments of Anatomy & Physiology and Kinesiology, Kansas State University, Manhattan, Kansas

Abstract

In contrast to cardiomyocytes, store overload-induced calcium ion (Ca^{2+}) release (SOICR) is not considered to constitute a primary Ca^{2+} releasing system from the sarcoplasmic reticulum (SR) in skeletal muscle myocytes. In the latter, voltage-induced Ca^{2+} release (VICR) is regarded as the dominant mechanism facilitating contractions. Any role of the SOICR in the regulation of cytoplasmic Ca^{2+} concentration ($[Ca^{2+}]_i$) and its dynamics in skeletal muscle in vivo remains poorly understood. By means of in vivo single fiber Ca^{2+} microinjections combined with bioimaging techniques, we tested the hypothesis that the $[Ca^{2+}]_i$ dynamics following Ca^{2+} injection would be amplified and fiber contraction facilitated by SOICR. The circulation-intact spinotrapezius muscle of adult male Wistar rats ($n = 34$) was exteriorized and loaded with Fura-2 AM to monitor $[Ca^{2+}]_i$ dynamics. Groups of rats underwent the following treatments: (1) 0.02, 0.2, and 2.0 mmol/L Ca^{2+} injections, (2) 2.0 mmol/L Ca^{2+} with inhibition of ryanodine receptors (RyR) by dantrolene sodium (DAN), and (3) 2.0 mmol/L Ca^{2+} with inhibition of SR Ca^{2+} ATPase (SERCA) by cyclopiazonic acid (CPA). A quantity of 0.02 mmol/L Ca^{2+} injection yielded no detectable response, whereas peak evoked $[Ca^{2+}]_i$ increased $9.9 \pm 1.8\%$ above baseline for 0.2 mmol/L and $23.8 \pm 4.3\%$ ($P < 0.05$) for 2.0 mmol/L Ca^{2+} injections. The peak $[Ca^{2+}]_i$ in response to 2.0 mmol/L Ca^{2+} injection was largely abolished by DAN and CPA (-85.8%, -71.0%, respectively, both $P < 0.05$ vs. unblocked) supporting dependence of the $[Ca^{2+}]_i$ dynamics on Ca^{2+} released by SOICR rather than injected Ca^{2+} itself. Thus, this investigation demonstrates the presence of a robust SR-evoked SOICR operant in skeletal muscle in vivo.

Introduction

Precise control of cytoplasmic calcium ion concentration ($[Ca^{2+}]_i$) is crucial for regulation of myocyte function and the excitation–contraction (E–C) coupling process in particular. In skeletal muscle myocytes, contraction and relaxation are evoked by $[Ca^{2+}]_i$ increase and decrease, respectively. The primary Ca^{2+} releasing systems from the sarcoplasmic reticulum (SR) are action potential-induced calcium release (voltage-induced Ca^{2+} release; VICR) (Schneider 1994; Hernandez-Ochoa et al. 2015), Ca^{2+}-induced Ca^{2+} release (CICR) (Endo 2009) and store

overload-induced Ca^{2+} release (SOICR) (Kong et al. 2007; Prakriya and Lewis 2015).

The ryanodine receptor (RyR) is a Ca^{2+} releasing channel on the SR membrane. In mammals, three RyR isoforms exist (RyR1, RyR2 and RyR3) with RyR1 being dominantly expressed in skeletal (Nakai et al. 1990; Otsu et al. 1990; Zorzato et al. 1990) as opposed to RyR2 in cardiac muscle (Nakai et al. 1990; Otsu et al. 1990; Zorzato et al. 1990). RyR3, discovered initially in the brain, also is present in the skeletal muscle (Giannini et al.

1995). However, RyR3 expression disappears in hind limb muscles of adult animals (Flucher et al. 1999). RyR is opened by interaction with the dihydropyridine receptor (DHPR), which is the voltage-dependent Ca^{2+} channel of the transverse tubule membrane (Lanner et al. 2010). Myocardial RyR2 causes Ca^{2+} release by binding with the Ca^{2+} which flows into the cytosol across the sarcolemma (Fabiato 1992; Maack and O'Rourke 2007). In marked contrast, skeletal muscle RyR1 is opened by the structural change in the RyR1-DHPR conjugate (Beam and Bannister 2010). Because this opening occurs in the absence of Ca^{2+} influx from the extracellular space, unlike that for cardiomyocytes, it is thought that a rise in $[Ca^{2+}]_i$ is not necessary for RyR1-mediated SR Ca^{2+} release. However, not all SR RyR1 is in contact with DHPR. Thus, the presence of non-DHPR-associated RyR1 in skeletal muscle myocytes raises the possibility that these particular RyR1's may release Ca^{2+} in a process instigated by Ca^{2+} that is released from the conjugated DHPR-RyR1 (Klein and Schneider 2006; Pouvreau et al. 2007; Van Petegem 2012).

Although SOICR is well known to operate via RyR2 in cardiomyocytes, it has never been observed for RyR1-bearing skeletal muscle myocytes even under conditions propagating Ca^{2+}release via the SR (Zhou et al. 2004; Figueroa et al. 2012). Interestingly, however, the Ca^{2+} sensing gate on the RyR for SOICR has been identified as a common gating structure for all RyR isoforms (Chen et al. 2014) and Ca^{2+} release via SOICR does occur in skeletal muscle myocytes similar to cardiac myocytes expressing RyR2 (Cully et al. 2014). In addition, reduction of Ca^{2+} entry across the sarcolemma reduces SR Ca^{2+} accumulation and induces muscle fatigue (Stiber et al. 2008). Collectively, these findings suggest that Ca^{2+} release by SOICR might play an important role in skeletal muscle in vivo.

Because RyR regulation is extremely sensitive to the cytosolic and luminal environments, and changes thereof (Laver et al. 2000; Fill and Coppell 2002; Capes et al. 2011), direct evidence for the presence of SOICR must be obtained under in vivo conditions especially as regards pH, temperature, reactive O_2 species, and O_2 partial pressure. The present investigation was designed to resolve the presence and putative importance of SOICR in an in vivo skeletal muscle using Ca^{2+} solutions injected directly into the myocyte cytosol which bypasses the VICR process entirely. We hypothesized that the $[Ca^{2+}]_i$ change in response to the Ca^{2+} solution injection would be amplified by SOICR, raising $[Ca^{2+}]_i$ substantially and causing muscle contraction. Furthermore, it was hypothesized that this amplification would be either abolished or reduced when Ca^{2+} release from the SR is inhibited, either directly via the blockade of RyR by the hydantoin

derivative dantrolene (DAN), or indirectly via the depletion of Ca^{2+} from the SR by inhibiting SERCA with cyclopiazonic acid (CPA).

Methods

Animals

Male Wistar rats ($n = 34$, 10–14 weeks of age; Japan SLC, Shizuoka, Japan) were used in this study. Rats were maintained on a 12:12-h light/dark cycle and received food and water ad libitum. All experiments were conducted under the guidelines established by the Physiological Society of Japan and were approved by the University of Electro-Communications Institutional Animal Care and Use Committee. The rats were anesthetized using pentobarbital sodium (60 mg/kg i.p.), and supplemental doses of anesthesia were administered as needed. At the end of the experimental protocols, animals were killed by pentobarbital sodium overdose.

Muscle preparation

All experimental techniques, including the spinotrapezius muscle preparation, were performed, as described previously (Sonobe et al. 2008; Eshima et al. 2013). Briefly, the right spinotrapezius muscle was gently exteriorized with minimal blood loss and tissue/microcirculatory damage, and attached to a wire horseshoe around the caudal periphery by six equidistant sutures placed around the muscle perimeter. The exposed muscle tissue was kept moist by superfusing with warmed Krebs–Henseleit buffer (KHB; 132 mmol/L NaCl, 4.7 mmol/L KCl, 21.8 mmol/L $NaHCO_3$, 2.0 mmol/L $MgSO_4$, and 2.0 mmol/L $CaCl_2$) equilibrated with 95% N_2-5% CO_2 and adjusted to pH 7.4, at 37°C. The fluorescent Ca^{2+} indicator Fura-2 AM (5 mmol/L; Dojindo Laboratories, Kumamoto, Japan) was dissolved in dimethyl sulfoxide (DMSO) and Pluronic F-127 and dispersed into KHB solution at a final concentration of 40 μmol/L. The muscles were incubated in Fura-2 AM/KHB solution for 60 min on a 37°C hot plate (Kitazato Supply, Shizuoka, Japan). After incubation, muscles were rinsed with dye-free KHB solution to remove nonloaded Fura-2 AM.

In vivo image analysis

The spinotrapezius muscles loaded with Fura-2 AM were mounted on the 37°C glass hot plate and observed by fluorescence microscopy using a 10 × objective lens (0.30 numerical aperture; Nikon, Tokyo, Japan). After ensuring that the spinotrapezius muscle was not grossly damaged and supported robust capillary blood flow, a sampling

area ($\sim$880 $\times$ 663 μm) was selected, and bright-field images were captured. Thereafter, 340 and 380 nm wavelength excitation light was delivered using a Xenon lamp equipped with appropriate fluorescent filters, and pairs of fluorescence images were captured through the 510 nm emission wavelength filter for ratiometry (Roe et al. 1990). The fluorescence intensity of serial ratio images was normalized to the starting point (i.e., precondition, R0) of each experiment (R/R0).

Experimental Protocols

In vivo injection of Ca²⁺ solution

Capillary micropipettes were generated with a tip of 5 μm in diameter, which was achieved by custom grinding and inserted into the selected single muscle fiber using a micromanipulator precision-controlled advancer (MMO-220A; Narishige, Tokyo, Japan). Subsequently, using a microinjector (IM300; Narishige, Tokyo, Japan), a single muscle fiber was microinjected with 0.02, 0.2, and 2.0 mmol/L Ca²⁺ solution by microinjection at 35 psi (24,000 Pa) for 1 sec ($\sim$0.78 $\times$ 10^{-3} μL) (Tanaka et al. 2016). We used a piezoassisted micromanipulation system for perforation of the cell membrane (PiezoXpert; Eppendorf, Hamburg, Germany). The injection solution was adjusted using a mixture of Ca²⁺-free solution (KCl: 145 mmol/L, NaCl: 3.5 mmol/L, MgCl$_2$: 10 mmol/L, NaOH: 6.5 mmol/L, HEPES: 10 mmol/L) and the Ca²⁺ solution (CaCl$_2$·2H$_2$O: 10 mmol/L). Criteria for successful injection included an unchanged [Ca²⁺]$_i$ in adjacent muscle fibers. Fluorescence images were captured by a high-sensitivity CCD (charge-coupled device) digital camera (ORCA-Flash2.8; Hamamatsu Photonics, Hamamatsu, Japan) using image-capture software (NIS-Elements Advanced Research; Nikon, Tokyo, Japan) for 60 sec after injection. The scan requirements were set at 300–800 msec/image. We confirmed that insertion of the capillary micropipette itself and injection of Ca²⁺-free solution did not induce any [Ca²⁺]$_i$ change. The specific region of interest (ROI, width: 20 μm, height: 80% of muscle fiber diameter) for the Ca²⁺ measurement was set at a distance of 40 μm from the injection point. All experiments were performed with the rat's body temperature maintained at 37–38°C with the exteriorized muscles mounted on the 37°C glass hotplate.

Pharmacologic block of the SR function

Pharmacological agents DAN and CPA were purchased from Sigma-Aldrich (St. Louis, MO). DAN inhibits single ryanodine receptor (RyR) Ca²⁺ release channels (Kobayashi et al. 2005; Oo et al. 2015). CPA is a highly specific

and potent SERCA inhibitor (Seidler et al. 1989). Each inhibitor was dissolved in DMSO and diluted with KHB (DAN: 100 and 500 μmol/L, CPA: 10, 50, and 100 μmol/L) and the pharmacological action was confirmed by constructing dose–response curves. Based upon these studies, following Fura-2 incubation and rinse, DAN (100 μmol/L) or CPA (100 μmol/L) was applied for 5 min before the start of experiments. Subsequently, a single muscle fiber was microinjected with either of the 0.02, 0.2, and 2.0 mmol/L Ca²⁺ solution.

In vivo injection of caffeine solution

This protocol was the same as for the Ca²⁺ injection. The caffeine solution (100 μmol/L) was injected into each single muscle fiber both with and without DAN conditions.

Evaluation of the muscle fiber length

The muscle fiber shortening (i.e., contraction rate) was calculated frame-by-frame using autologous fluorescent landmarks, located close to the injection point and thus ~40 μm from the ROI. The resolution was 0.73 μm per pixel.

Statistical analysis

All experimental data are expressed as means $\pm$ SE. All statistical analyses were performed in Prism version 6.0 (GraphPad Software, San Diego, CA). Comparisons among different groups were analyzed by either one-way or two-way ANOVA followed by Tukey's multiple-comparison test. The level of significance was set at $P < 0.05$ (two-tailed).

Results

In contrast to the Ca²⁺-free and 0.02 mmol/L Ca²⁺ injections which caused no detectable [Ca²⁺]$_i$ change, 0.2 and 2.0 mmol/L injections elicited significant increases in [Ca²⁺]$_i$, indicated by 9.9 $\pm$ 1.8% and 23.8 $\pm$ 4.3% increases in R/R0 within 1–2 sec after injection, respectively (both $P < 0.0001$, two-way ANOVA, Figs. 1, 2). Interestingly, the [Ca²⁺]$_i$ increase declined subsequently but [Ca²⁺]$_i$ did not return to resting levels within the 60 sec observation period.

The functional concentrations of each inhibitor (DAN and CPA) were verified under in vivo conditions before Ca²⁺ injection (Fig. 3A). As evident from Figure 3B, the increment of [Ca²⁺]$_i$ with Ca²⁺ injection was barely detectable after DAN treatment (2.0 mmol/L: 3.4 $\pm$ 1.2%, 0.2 mmol/L: 3.6 $\pm$ 0.8%, 0.02 mmol/L: 1.9 $\pm$ 0.7% vs. unblocked control). With
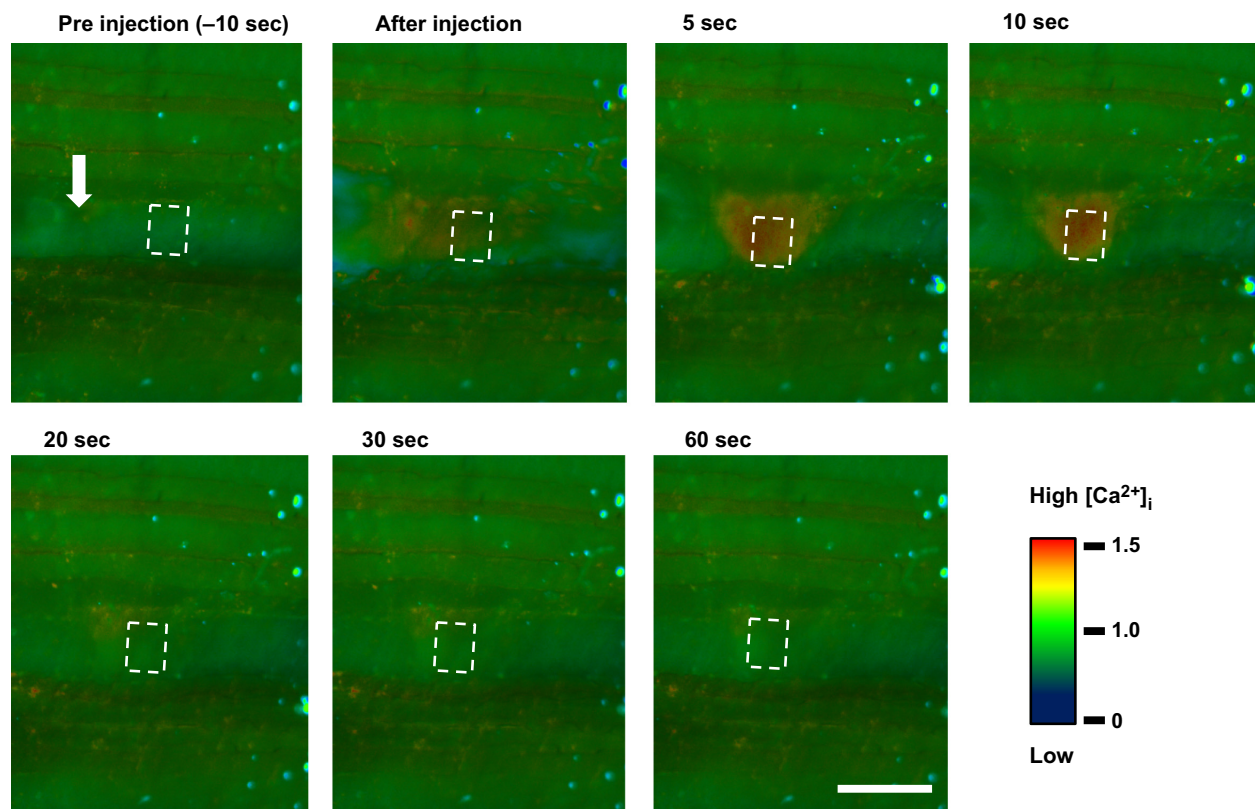
Figure 1. Representative example of changes in intracellular Ca²⁺ concentration ($[Ca^{2+}]_i$) induced by 2.0 mmol/L Ca²⁺ microinjection into a single rat spinotrapezius muscle myocyte. The injection site is shown with an arrow. The specific region of interest (width: 20 μm, height: 80% of muscle fiber diameter) for the Ca²⁺ measurement was set to a distance of 40 μm from the injection point. Scale bar = 50 μm. Pseudocolor bar indicates the 340/380-nm ratio value.

CPA-induced SERCA blockade, the $[Ca^{2+}]_i$ increase after injection was substantially blunted compared with the unblocked control condition (i.e., control 2.0 mmol/L Ca²⁺ injection, $23.8 \pm 4.3\%$ vs. CPA, $5.3 \pm 1.0\%$, $P < 0.05$).

Caffeine injection induced a $13.8 \pm 2.6\%$ $[Ca^{2+}]_i$ increase above baseline (Fig. 4). Unlike the 0.2 mmol/L and 2.0 mmol/L injectates, this $[Ca^{2+}]_i$ increase resolved to baseline within 60 sec (compare Figs. 2, 4). DAN blockade of RyR almost completely abolished the caffeine-induced $[Ca^{2+}]_i$ increase (Fig. 4).

2.0 mmol/L Ca²⁺ injection induced a rapid (peak velocity, 43.0 ± 11.0 μm/sec) and substantial (peak shortening length, 89.5 ± 15.1 μm, mean shortening length 48.0 ± 7.7 μm) fiber shortening as seen in Figure 5. Two-way repeated-measures analyses revealed a significant effect for DAN ($P < 0.03$, vs. Ca²⁺ alone condition) and CPA ($P < 0.03$, vs. Ca²⁺ alone condition) on shortening fiber length. Specifically, the mean shortening length was significantly reduced in both DAN (25.1 ± 6.6 μm) and CPA (14.4 ± 4.0 μm) compared with 2.0 mmol/L Ca²⁺ alone (Fig. 5D).

For the caffeine condition, compared with the 2.0 mmol/L Ca²⁺ injection, there was a strong tendency for a reduced shortening (22.9 ± 4.6 μm, $P = 0.059$, Fig. 5D) and a slower velocity of shortening (16.3 ± 2.5 μm/sec, $P = 0.060$, Fig. 5C).

Discussion

This investigation represents the first in vivo imaging of $[Ca^{2+}]_i$ dynamics associated with direct single fiber Ca²⁺ loading in an in vivo skeletal muscle of rats. The principal original finding was that the $[Ca^{2+}]_i$ dynamics following Ca²⁺ injection reflect Ca²⁺ released by SOICR rather than the effects of the injected Ca²⁺ itself. This schema is supported by the almost complete abolition of $[Ca^{2+}]_i$ increase consequent to RyR and SERCA inhibition.

$[Ca^{2+}]_i$ response to Ca²⁺ injection

In the absence of intramyocyte (e.g., troponin) Ca²⁺ binding as well as SR release and sequestration processes the change in $[Ca^{2+}]_i$ should directly reflect the amount
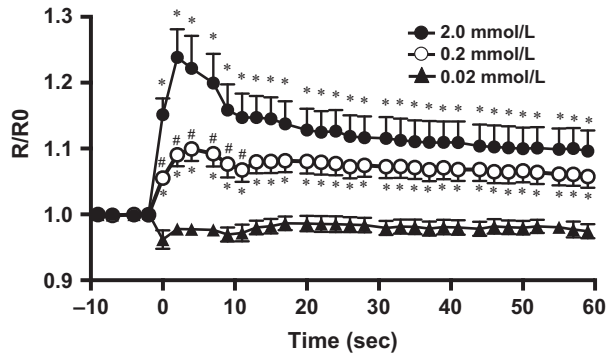
Figure 2. Influence of the different Ca²⁺ injections (0.02, 0.2 2.0 mmol/L) on intracellular Ca²⁺ concentration ([Ca²⁺]ᵢ) in vivo. Fluorescence was measured continuously during the 60 sec measurement interval and ratiometrically quantified data were graphed as changes from precondition (i.e. −10 sec) levels (R0). Values shown are means ± SE ($N = 10$, 0.02 mmol/L: $n = 14$, 0.2 mmol/L: $n = 17$, 2.0 mmol/L: $n = 17$). N = number of animals. n = number of muscle fibers measured. There was a significant interaction effect for treatment condition (0.02, 0.2 and 2.0 mmol/L) and time course of injection ($P < 0.001$). Significant difference between each conditions for the same time points: *$P < 0.05$ (vs. 0.02 mmol/L), #$P < 0.05$ (vs. 2.0 mmol/L).

of injected Ca²⁺ within the cytoplasmic distribution volume. For instance, in a myocyte that has a 60 μm diameter and length 700 μm, the volume will be approximately 2.0×10^{-3} μL. When 0.78×10^{-3} μL of 0.02, 0.2, and

2.0 mmol/L Ca²⁺ solution was injected, it is estimated that the [Ca²⁺]ᵢ will increase to 0.0057, 0.057, and 0.57 mmol/L, respectively. As can be seen from Figures 2 and 3, however, there was no proportional relationship between injected [Ca²⁺] and the resultant rise in [Ca²⁺]ᵢ, providing evidence for the presence of a complex Ca²⁺ homeostasis system. That the 0.02 mmol/L injection did not elevate [Ca²⁺]ᵢ indicates that either any [Ca²⁺]ᵢ increase was below the sensitivity of our detection system or, alternatively, the injected Ca²⁺ was removed by Ca²⁺-troponin binding and/or sequestration processes by SR and mitochondria. In contrast, both 0.2 mmol/L and 2.0 mmol/L injections invoked a rapid and substantial increase in [Ca²⁺]ᵢ (Fig. 2) that was almost entirely prevented by either RyR (DAN) or SERCA (CPA) inhibition (Fig. 3). This observation provides strong evidence that a functional and robust SOICR is present in rat myocytes in vivo.

Ca²⁺ itself modulates RyR channel activity (Gehlert et al. 2015) being stimulatory at low Ca²⁺ (~1 μmol/L) and inhibitory at extremely high Ca²⁺ (~1 mmol/L) (Meissner 1986). DAN inhibits skeletal muscle L-type Ca²⁺ currents by disrupting communication between RyR1 and Ca(V)1 which provides the only treatment for malignant hyperthermia resulting from RyR1 mutations (Zhao et al. 2001; Bannister 2013). Although the precise molecular mechanism(s) for DAN's RyR1 functional action remain to be defined (Nelson et al. 1996; Oo et al.
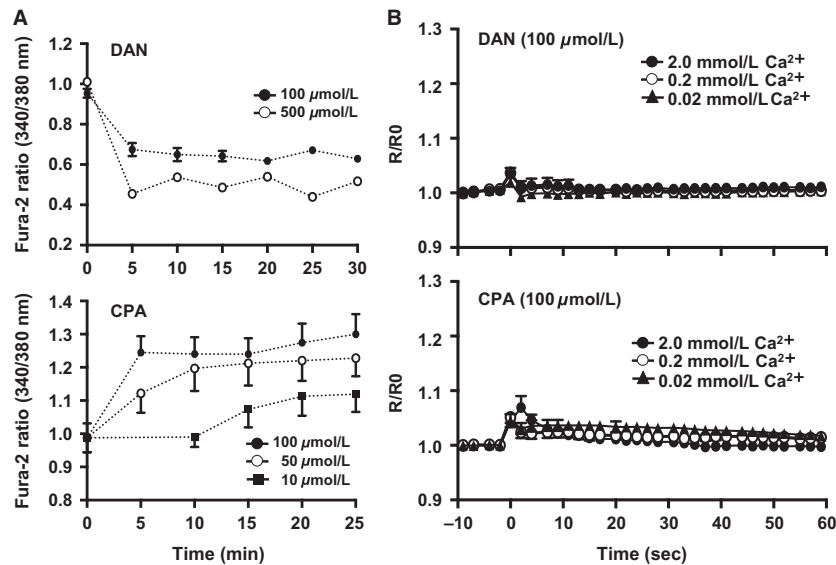
Figure 3. (A) The dose–response curves show the pharmacologic function of DAN (100, 500 μmol/L) and CPA (10, 50, 100 μmol/L) in the in vivo environment. (B) Influence of the DAN, top panel and CPA, bottom panel in vivo on intracellular Ca²⁺ concentration ([Ca²⁺]ᵢ). Values shown are means ± SE (DAN condition: $N = 7$, 0.02 mmol/L: $n = 14$, 0.2 mmol/L: $n = 18$, 2.0 mmol/L: $n = 18$, CPA condition: $N = 7$, 0.02 mmol/L: $n = 15$, 0.2 mmol/L: $n = 15$, 2.0 mmol/L: $n = 15$). N = number of animals. n = number of muscle fibers measured. CPA, cyclopiazonic acid; DAN, dantrolene sodium.
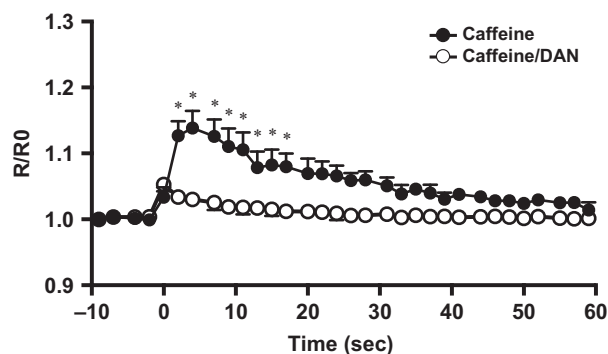
Figure 4. Influence of caffeine injection with/without DAN in vivo on intracellular Ca^{2+} concentration ($[Ca^{2+}]_i$). Values shown are means $\pm$ SE (caffeine condition: $N = 5$, $n = 9$, caffeine/DAN condition: $N = 5$, $n = 8$). N = number of animals. n = number of muscle fibers measured. There was a significant interaction effect for treatment condition (caffeine injection with/without DAN) and time course of injection ($P < 0.001$). Significant difference between each condition at the same time point: $*P < 0.05$ (caffeine injection with vs. without DAN). DAN, dantrolene sodium.

2015), discrete findings within isolated muscle and skinned muscle fibers offer pertinent clues. For instance, in E–C coupling, DAN diminishes the twitch tension much more than the tetanic tension (Leslie and Part 1981) and both reduced temperatures (22°C) (Ohta et al. 1990; Krause et al. 2004; Kobayashi et al. 2005) and the presence of Mg^{2+} (Ohta et al. 1990; Owen et al. 1997) impair DAN's ability to inhibit RyR1. Unfortunately, as mentioned in the Introduction, in vitro conditions present in those investigations are expected, in and of themselves, to perturb $[Ca^{2+}]_i$ and RyR regulation. Specifically, RyR is a redox-sensitive channel and myocyte redox regulation is dependent on O_2 (and thus O_2 partial pressure, PO_2) (Salama et al. 2000; Powers et al. 2011). Although physiological microvascular PO_2 are 20–30 Torr in the in vivo spinotrapezius muscle (Kano et al. 2005) and intramyocyte PO_2 must be even lower, studies of isolated skeletal muscles are routinely performed in hyperoxic environments (95% O_2, >600 Torr). This realization tempers confidence in translating ex vivo findings to the in vivo environment. Notwithstanding this consideration, the present investigation has extended previous observations regarding $[Ca^{2+}]_i$ control and represents the first investigation to provide evidence for SOICR function in vivo.

The effects of RyR and SERCA inhibition on the $[Ca^{2+}]_i$ response and contractile function

We hypothesized that SOICR function would be abolished when Ca^{2+} release from the SR is inhibited, either directly via the blockade of RyR (DAN), or indirectly via the depletion of Ca^{2+} from the SR (CPA). This hypothesis was supported by the almost complete abolition of $[Ca^{2+}]_i$ increases by DAN and CPA applied separately.

SOICR has been observed in RyR2 containing cardiomyocytes (Diaz et al. 1997; Eisner et al. 2009) and occurs consequent to RyR opening when the stored Ca^{2+} content exceeds some threshold level. SOICR has been observed for RYR1 in skeletal muscle myocytes as well as RyR3 in smooth muscle (Chen et al. 2014). As we added an additional Ca^{2+} load to the myocytes, we considered this to be the basis for triggering SOICR. Recently, Cully and colleague observed in rodent skinned fibers that a local $[Ca^{2+}]_i$ increase via SOICR was propagated by movement of Ca^{2+} inside the SR (Cully et al. 2014). A similar phenomenon was identified in rabbit ventricular myocytes where local SR Ca^{2+} uptake by SERCA facilitated propagation of cytosolic Ca^{2+} waves via luminal sensitization of the RyR (Maxwell and Blatter 2012). These cytoplasmic Ca^{2+} waves can be explained by discrete fluctuations of Ca^{2+} inside the SR network. In the present investigation, we have demonstrated that, following injection of 0.2 and 2.0 mmol/L Ca^{2+} solution, pharmacologic inhibition of SR Ca^{2+} release by DAN and uptake by CPA largely, but not totally, prevented subsequent $[Ca^{2+}]_i$ increase (Fig. 3, lower panel). As injected Ca^{2+} would be instantly sequestered by SERCA, when allowed to function normally (i.e., absence of CPA) this would acutely increase net SR Ca^{2+} stores. Consequently, local Ca^{2+} release following Ca^{2+} injection would be triggered by the SOICR system and contribute to the contractile behavior evident in Figure 5. Interestingly, even in the presence of DAN or CPA 40–60% of the control muscle contractile response (extent of shortening and shortening velocity) was preserved. The most likely explanation for this behavior is that the injected Ca^{2+} bound immediately to troponin and directly facilitated contraction.

Consideration of the experimental model

We examined Ca^{2+} release with caffeine to confirm the physiological response of the in vivo experimental model. Caffeine increases the sensitivity of RyR for Ca^{2+} (Rousseau et al. 1988; Zucchi and Ronca-Testoni 1997; Murayama et al. 2000) and caffeine-induced Ca^{2+} transients are evident in myotubes and adult skeletal muscle (Endo et al. 1970; Horiuti 1988; Lamb et al. 2001). In this study, under the in vivo control condition, there was a significant increase in $[Ca^{2+}]_i$ after caffeine injection, and this was markedly attenuated by DAN (Fig. 4). That Ca^{2+} release by caffeine could be inhibited by DAN provides additional evidence that the Ca^{2+} release via SR is present and functional in vivo. Also, the muscle contraction
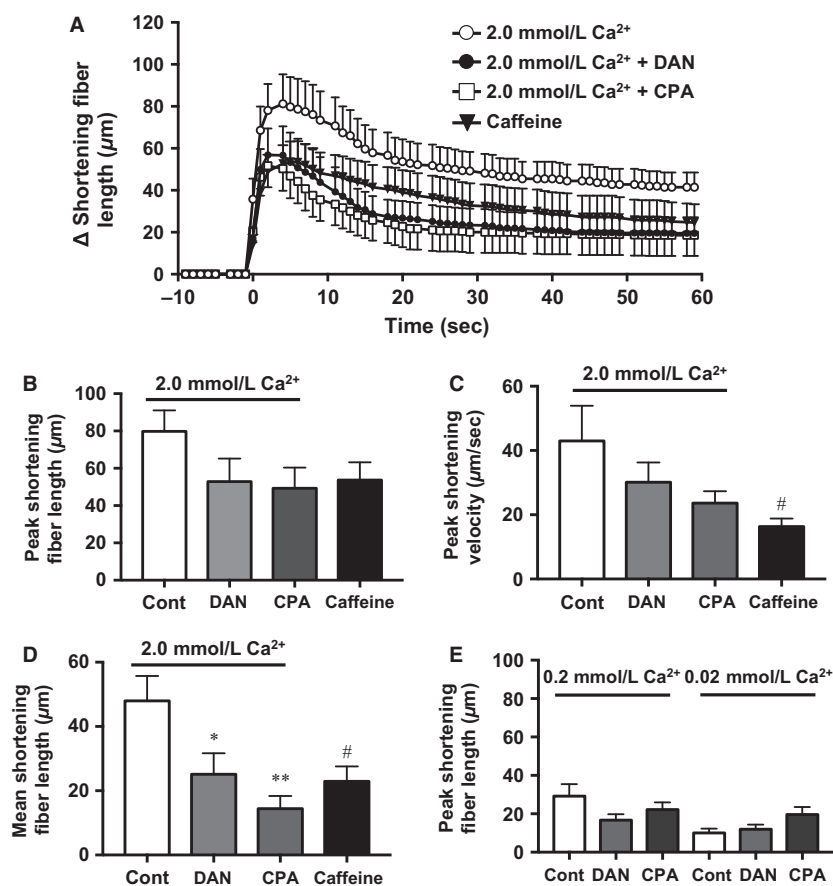
Figure 5. (A) Changes of muscle fiber length (i.e., extent of shortening) during each injection protocol (Ca²⁺, Ca²⁺+DAN, Ca²⁺+CPA, and caffeine). Values shown are means ± SE (Ca²⁺: *n* = 12, Ca²⁺+DAN: *n* = 14 Ca²⁺+CPA: *n* = 15, caffeine: *n* = 9). *n* = number of muscle fibers measured. B, C, and D: Shortening dynamics at 2.0 mmol/L Ca²⁺ and caffeine injection. (B) Bar graph shows peak shortening length. There was no statistically significant difference among conditions. (C) Bar graph shows peak shorting velocity. The Caffeine condition tended to be slower than 2.0 mmol/L Ca²⁺ control (#*P* = 0.060). (D) Bar graph shows mean fiber length shortening during 60 sec following injection. Significance compared with Ca²⁺ condition, **P* < 0.05, ***P* < 0.01. The Caffeine condition tended to be shorter than the Ca²⁺ condition (#*P* = 0.059). (E) Bar graph shows peak shortening length for 0.2 mmol/L and 0.02 mmol/L Ca²⁺ conditions. Significant changes with the inhibitors were not found in either Ca²⁺ concentration conditions. CPA, cyclopiazonic acid; DAN, dantrolene sodium.

induced by caffeine injection is most likely the result of RyR-released Ca²⁺. The peak shortening velocity and extent of fiber shortening with caffeine tended to be slower and reduced compared with the control Ca²⁺ condition ($P = 0.06$, Fig. 5 panel C) which might be associated with inertia in the Ca²⁺ release system resulting from caffeine-induced RyR sensitization. Under these circumstances, it would be expected that the SOICR Ca²⁺ release rate would be far slower than VICR. However, resolution of the mechanistic basis for this behavior will require more precise temporal measurements of the contractile response than attempted, or possible, herein.

The $[Ca^{2+}]_i$ in mammalian myocyte is around 20–50 nmol/L under resting conditions, while the peak $[Ca^{2+}]_i$ increases to the low μmol/L level during tetanic stimulation (Allen and Westerblad 2001). Computational

modeling estimates that the total released SR Ca²⁺ is around 0.35 mmol/L during tetanic stimulation in intact fast-twitch mouse myocytes (Baylor and Hollingworth 2003). It is quite possible therefore that the local injection of 2.0 mmol/L Ca²⁺ may be beyond the range seen physiologically. Although highly concentrated Ca²⁺ (~1 mmol/L) has been shown to inhibit rather than facilitate RyR function (Meissner 1986), the present results clearly demonstrate facilitation of RyR Ca²⁺ release. Therefore, even though we elected to inject 2.0 mmol/L Ca²⁺ the volume was extremely small (0.78 nL) and the resultant free $[Ca^{2+}]_i$ is expected to be reduced immediately by intramyocyte buffering mechanisms and dilution within the far larger cytosolic volume.

Mg²⁺, Zn²⁺, NO, and ATP are known modulators of the RyR function (Xia et al. 2000; Lanner et al.

2010; Suhr et al. 2013) and perturbations in the concentrations of these molecules, and therefore Ca^{2+} regulation, is inevitable when the in vivo myocyte environment is lost. For instance, the ATP requirement for the SR Ca^{2+} pumping, required to maintain Ca^{2+} homeostasis, demands up to 40–50% of resting cellular energy consumption (Smith et al. 2013). Even if it is possible to provide sufficient O_2 in vitro to sustain this activity disruption of the intracellular PO_2 (by hyperoxia and/or hypoxia) will invariably alter metabolic regulation, intramyocyte redox and the intramyocyte milieu (e.g., (Hogan et al. 1992; Wilson et al. 1977). This consideration demands careful interpretation of in vitro data when applying them to in vivo physiological mechanisms and is especially pertinent for understanding in vivo muscle Ca^{2+} homeostasis. A signatory advantage of the present investigation is having a preparation that maintains close-to-physiological intramyocyte homeostasis especially as regards ion balance and energy supply.

In conclusion, in the absence of VICR, we demonstrated, for the first time, evidence for SR SOICR in in vivo single mammalian skeletal muscle myocytes. The SOICR demonstrated induced elevated $[Ca^{2+}]_i$ and significant myocyte shortening; both of which were diminished substantially by RyR blockade or SERCA inhibition.

Conflict of Interest

None declared.

References

Allen, D. G., and H. Westerblad. 2001. Role of phosphate and calcium stores in muscle fatigue. J. Physiol. 536:657–665.

Bannister, R. A. 2013. Dantrolene-induced inhibition of skeletal L-type Ca^{2+} current requires RyR1 expression. Biomed. Res. Int. 2013:390493.

Baylor, S. M., and S. Hollingworth. 2003. Sarcoplasmic reticulum calcium release compared in slow-twitch and fast-twitch fibres of mouse muscle. J. Physiol. 551:125–138.

Beam, K. G., and R. A. Bannister. 2010. Looking for answers to EC coupling's persistent questions. J. Gen. Physiol. 136:7–12.

Capes, E. M., R. Loaiza, and H. H. Valdivia. 2011. Ryanodine receptors. Skelet. Muscle 1:18.

Chen, W., R. Wang, B. Chen, X. Zhong, H. Kong, Y. Bai, et al. 2014. The ryanodine receptor store-sensing gate controls Ca^{2+} waves and Ca^{2+}-triggered arrhythmias. Nat. Med. 20:184–192.

Cully, T. R., J. N. Edwards, and B. S. Launikonis. 2014. Activation and propagation of Ca^{2+} release from inside the sarcoplasmic reticulum network of mammalian skeletal muscle. J. Physiol. 592:3727–3746.

Diaz, M. E., A. W. Trafford, S. C. O'Neill, and D. A. Eisner. 1997. Measurement of sarcoplasmic reticulum Ca^{2+} content and sarcolemmal Ca^{2+} fluxes in isolated rat ventricular myocytes during spontaneous Ca^{2+} release. J. Physiol. 501:3–16.

Eisner, D. A., T. Kashimura, L. A. Venetucci, and A. W. Trafford. 2009. From the ryanodine receptor to cardiac arrhythmias. Circ. J. 73:1561–1567.

Endo, M. 2009. Calcium-induced calcium release in skeletal muscle. Physiol. Rev. 89:1153–1176.

Endo, M., M. Tanaka, and Y. Ogawa. 1970. Calcium induced release of calcium from the sarcoplasmic reticulum of skinned skeletal muscle fibres. Nature 228:34–36.

Eshima, H., Y. Tanaka, T. Sonobe, T. Inagaki, T. Nakajima, D. C. Poole, et al. 2013. In vivo imaging of intracellular Ca^{2+} after muscle contractions and direct Ca^{2+} injection in rat skeletal muscle in diabetes. Am. J. Physiol. Regul. Integr. Comp. Physiol. 305:R610–R618.

Fabiato, A. 1992. 2 Kinds of calcium-induced release of calcium from the sarcoplasmic reticulum of skinned cardiac cells. Adv. Exp. Med. Biol. 311:245–262.

Figueroa, L., V. M. Shkryl, J. Zhou, C. Manno, A. Momotake, G. Brum, et al. 2012. Synthetic localized calcium transients directly probe signalling mechanisms in skeletal muscle. J. Physiol. 590:1389–1411.

Fill, M., and J. A. Copello. 2002. Ryanodine receptor calcium release channels. Physiol. Rev. 82:893–922.

Flucher, B. E., A. Conti, H. Takeshima, and V. Sorrentino. 1999. Type 3 and type 1 ryanodine receptors are localized in triads of the same mammalian skeletal muscle fibers. J. Cell Biol. 146:621–630.

Gehlert, S., W. Bloch, and F. Suhr. 2015. Ca^{2+}-dependent regulations and signaling in skeletal muscle: from electro-mechanical coupling to adaptation. Int. J. Mol. Sci. 16:1066–1095.

Giannini, G., A. Conti, S. Mammarella, M. Scrobogna, and V. Sorrentino. 1995. The ryanodine receptor/calcium channel genes are widely and differentially expressed in marine brain and peripheral tissues. J. Cell Biol. 128:893–904.

Hernandez-Ochoa, E. O., S. J. Pratt, R. M. Lovering, and M. F. Schneider. 2015. Critical role of intracellular RyR1 calcium release channels in skeletal muscle function and disease. Front. Physiol. 6:420.

Hogan, M. C., P. G. Arthur, D. E. Bebout, P. W. Hochachka, and P. D. Wagner. 1992. Role of O_2 in regulating tissue respiration in dog muscle working in situ. J. Appl. Physiol. 73: 728–736.

Horiuti, K. 1988. Mechanism of contracture on cooling of caffeine-treated frog skeletal muscle fibres. J. Physiol. 398:131–148.

Kano, Y., D. J. Padilla, B. J. Behnke, K. S. Hageman, T. I. Musch, and D. C. Poole. 2005. Effects of eccentric exercise on microcirculation and microvascular oxygen pressures in rat spinotrapezius muscle. J. Appl. Physiol. 99:1516–1522.

Klein, M. G., and M. F. Schneider. 2006. Ca²⁺ sparks in skeletal muscle. Prog. Biophys. Mol. Biol. 92:308–332.

Kobayashi, S., M. L. Bannister, J. P. Gangopadhyay, T. Hamada, J. Parness, and N. Ikemoto. 2005. Dantrolene stabilizes domain interactions within the ryanodine receptor. J. Biol. Chem. 280:6580–6587.

Kong, H. H., R. W. Wang, W. Q. Chen, L. Zhang, K. Y. Chen, Y. Shimoni, et al. 2007. Skeletal and cardiac ryanodine receptors exhibit different responses to Ca²⁺ overload and luminal Ca²⁺. Biophys. J. 92:2757–2770.

Krause, T., M. U. Gerbershagen, M. Fiege, R. Weisshorn, and F. Wappler. 2004. Dantrolene–a review of its pharmacology, therapeutic use and new developments. Anaesthesia 59:364–373.

Lamb, G. D., M. A. Cellini, and D. G. Stephenson. 2001. Different Ca²⁺ releasing action of caffeine and depolarisation in skeletal muscle fibres of the rat. J. Physiol. 531:715–728.

Lanner, J. T., D. K. Georgiou, A. D. Joshi, and S. L. Hamilton. 2010. Ryanodine receptors: structure, expression, molecular details, and function in calcium release. Cold Spring Harb. Perspect. Biol. 2:a003996.

Laver, D. R., K. R. Eager, L. Taoube, and G. D. Lamb. 2000. Effects of cytoplasmic and luminal pH on Ca²⁺ release channels from rabbit skeletal muscle. Biophys. J. 78:1835–1851.

Leslie, G. C., and N. J. Part. 1981. The action of dantrolene sodium on rat fast and slow muscle in vivo. Br. J. Pharmacol. 72:665–672.

Maack, C., and B. O'Rourke. 2007. Excitation-contraction coupling and mitochondrial energetics. Basic Res. Cardiol. 102:369–392.

Maxwell, J. T., and L. A. Blatter. 2012. Facilitation of cytosolic calcium wave propagation by local calcium uptake into the sarcoplasmic reticulum in cardiac myocytes. J. Physiol. 590:6037–6045.

Meissner, G. 1986. Ryanodine activation and inhibition of the Ca²⁺ release channel of sarcoplasmic reticulum. J. Biol. Chem. 261:6300–6306.

Murayama, T., N. Kurebayashi, and Y. Ogawa. 2000. Role of Mg²⁺ in Ca²⁺-induced Ca²⁺ release through ryanodine receptors of frog skeletal muscle: modulations by adenine nucleotides and caffeine. Biophys. J. 78:1810–1824.

Nakai, J., T. Imagawa, Y. Hakamat, M. Shigekawa, H. Takeshima, and S. Numa. 1990. Primary structure and functional expression from cDNA of the cardiac ryanodine receptor/calcium release channel. FEBS Lett. 271:169–177.

Nelson, T. E., M. Lin, G. Zapata-Sudo, and R. T. Sudo. 1996. Dantrolene sodium can increase or attenuate activity of skeletal muscle ryanodine receptor calcium release channel. Clinical implications. Anesthesiology 84:1368–1379.

Ohta, T., S. Ito, and A. Ohga. 1990. Inhibitory action of dantrolene on Ca²⁺-induced Ca²⁺ release from sarcoplasmic reticulum in guinea pig skeletal muscle. Eur. J. Pharmacol. 178:11–19.

Oo, Y. W., N. Gomez-Hurtado, K. Walweel, D. F. van Helden, M. S. Imtiaz, B. C. Knollmann, et al. 2015. Essential role of calmodulin in RyR inhibition by dantrolene. Mol. Pharmacol. 88:57–63.

Otsu, K., H. F. Willard, V. K. Khanna, F. Zorzato, N. M. Green, and D. H. MacLennan. 1990. Molecular cloning of cDNA encoding the Ca²⁺ release channel (ryanodine receptor) of rabbit cardiac muscle sarcoplasmic reticulum. J. Biol. Chem. 265:13472–13483.

Owen, V. J., N. L. Taske, and G. D. Lamb. 1997. Reduced Mg²⁺ inhibition of Ca²⁺ release in muscle fibers of pigs susceptible to malignant hyperthermia. Am. J. Physiol. 272: C203–C211.

Pouvreau, S., L. Royer, J. Yi, G. Brum, G. Meissner, E. Rios, et al. 2007. Ca²⁺ sparks operated by membrane depolarization require isoform 3 ryanodine receptor channels in skeletal muscle. Proc. Natl. Acad. Sci. USA 104:5235–5240.

Powers, S. K., L. L. Ji, A. N. Kavazis, and M. J. Jackson. 2011. Reactive oxygen species: impact on skeletal muscle. Compr. Physiol. 1:941–969.

Prakriya, M., and R. S. Lewis. 2015. Store-operated calcium channels. Physiol. Rev. 95:1383–1436.

Roe, M. W., J. J. Lemasters, and B. Herman. 1990. Assessment of Fura-2 for measurements of cytosolic free calcium. Cell Calcium 11:63–73.

Rousseau, E., J. Ladine, Q. Y. Liu, and G. Meissner. 1988. Activation of the Ca²⁺ release channel of skeletal muscle sarcoplasmic reticulum by caffeine and related compounds. Arch. Biochem. Biophys. 267:75–86.

Salama, G., E. V. Menshikova, and J. J. Abramson. 2000. Molecular interaction between nitric oxide and ryanodine receptors of skeletal and cardiac sarcoplasmic reticulum. Antioxid. Redox Signal. 2:5–16.

Schneider, M. F. 1994. Control of calcium release in functioning skeletal muscle fibers. Annu. Rev. Physiol. 56:463–484.

Seidler, N. W., I. Jona, M. Vegh, and A. Martonosi. 1989. Cyclopiazonic acid is a specific inhibitor of the Ca²⁺-ATPase of sarcoplasmic reticulum. J. Biol. Chem. 264:17816–17823.

Smith, I. C., E. Bombardier, C. Vigna, and A. R. Tupling. 2013. ATP consumption by sarcoplasmic reticulum Ca²⁺ pumps accounts for 40-50% of resting metabolic rate in mouse fast and slow twitch skeletal muscle. PLoS ONE 8:e68924.

Sonobe, T., T. Inagaki, D. C. Poole, and Y. Kano. 2008. Intracellular calcium accumulation following eccentric contractions in rat skeletal muscle in vivo: role of stretch-activated channels. Am. J. Physiol. Regul. Integr. Comp. Physiol. 294:R1329–R1337.

Stiber, J., A. Hawkins, Z. S. Zhang, S. Wang, J. Burch, V. Graham, et al. 2008. STIM1 signalling controls store-operated calcium entry required for development and contractile function in skeletal muscle. Nat. Cell Biol. 10:688–697.

Suhr, F., S. Gehlert, M. Grau, and W. Bloch. 2013. Skeletal muscle function during exercise-fine-tuning of diverse subsystems by nitric oxide. Int. J. Mol. Sci. 14:7109–7139.

Tanaka, Y., T. Inagaki, D. C. Poole, and Y. Kano. 2016. pH buffering of single rat skeletal muscle fibers in the in vivo environment. Am. J. Physiol. Regul. Integr. Comp. Physiol. 310:R926–R933.

Van Petegem, F. 2012. Ryanodine receptors: structure and function. J. Biol. Chem. 287:31624–31632.

Wilson, D. F., M. Erecinska, C. Drown, and I. A. Silver. 1977. Effect of oxygen tension on cellular energetics. Am. J. Physiol. 233:C135–C140.

Xia, R. H., X. Y. Cheng, H. Wang, K. Y. Chen, Q. Q. Wei, X. H. Zhang, et al. 2000. Biphasic modulation of ryanodine binding to sarcoplasmic reticulum vesicles of skeletal muscle by Zn^{2+} ions. Biochem. J. 345(Pt 2):279–286.

Zhao, F., P. Li, S. R. Chen, C. F. Louis, and B. R. Fruen. 2001. Dantrolene inhibition of ryanodine receptor Ca^{2+} release channels. Molecular mechanism and isoform selectivity. J. Biol. Chem. 276:13810–13816.

Zhou, J., B. S. Launikonis, E. Rios, and G. Brum. 2004. Regulation of Ca^{2+} sparks by Ca^{2+} and Mg^{2+} in mammalian and amphibian muscle. An RyR isoform-specific role in excitation-contraction coupling? J. Gen. Physiol. 124:409–428.

Zorzato, F., J. Fujii, K. Otsu, M. Phillips, N. M. Green, F. A. Lai, et al. 1990. Molecular cloning of cDNA encoding human and rabbit forms of the Ca^{2+} release channel (ryanodine receptor) of skeletal muscle sarcoplasmic reticulum. J. Biol. Chem. 265:2244–2256.

Zucchi, R., and S. Ronca-Testoni. 1997. The sarcoplasmic reticulum Ca^{2+} channel/ryanodine receptor: modulation by endogenous effectors, drugs and disease states. Pharmacol. Rev. 49:1–51.